

Waves Trapped To Discrete Topography: Existence and Implications

D.S. Luther

School of Ocean and Earth Science and Technology, University of Hawaii, Honolulu, Hawaii

Abstract. The characteristics of observed energetic waves trapped to discrete topographic features, especially islands and mid-ocean ridge segments, are discussed. Resonant oscillations may occur due to closed propagation paths or zero group velocity along isobaths. The waves are forced directly by fluctuating winds, and may also be forced indirectly through the atmosphere's excitation of open ocean waves that subsequently impinge upon the topography. Evidence of energy leakage from one resonant island trapped wave to a resonant wave trapped to a neighboring island is reviewed. The potential importance of the poorly understood island and ridge trapped waves to teleconnections, mixing at the water-earth boundary, effluent dispersal, and general circulation simulations is noted.

Introduction

Perhaps the most important characteristic of the ocean's many types of free waves is their ability to propagate information about a disturbance from the region of forcing to an otherwise quiescent distant location. Waveguides, produced for example by topography at a coast (e.g., yielding refractive trapping to the coast), or by the reversal of sign of the vertical Coriolis parameter at the equator (equatorially-trapped waves), etc., enhance this characteristic by reducing the energy loss that would otherwise occur if the wave were to propagate in all directions indiscriminately. The wave is focused in a particular direction so that its energy density is not diminished by dispersal in multiple directions. For example, long period waves (periods greater than a day) trapped to continental coastlines are now well respected for their impact on currents and temperature fields far from the point of origin (e.g., *Brink*, 1991). Long period waves trapped to the equator play a variety of roles in the onset and maturation of climatically significant phenomena by propagating information about atmospheric changes across ocean basins (e.g., the El Niño phenomenon; *Philander*, 1990).

This note reviews some wave types whose existence has received minimal attention in the literature, and whose impact has been noted only briefly but could be substantial in both the teleconnection sense outlined above and the local sense of how strong the ocean's response will be to imposed forcing. The waves in question are those trapped to discrete topography, by which is meant topography of limited extent, though this concept will not be made precise for this review. Such topographic features as islands, seamounts, ridge segments and plateaus enable many kinds of free waves to exist that are trapped to the topography in a stratified ocean and therefore are guided to freely propagate in (usually) only one direction, i.e., along isobaths.

The reason the scale of the 'discrete' topography will not be defined rigorously is that some of the more

interesting observations that have arisen lately are of waves trapped to a mid-ocean ridge segment, e.g., the Juan de Fuca Ridge. These waves raise the question of existence and propagation for long distances along the mid-ocean ridges. If a ridge-trapped wave were generated by a storm in the South Pacific Ocean could it propagate up to the equator along the East Pacific Rise? This paper will concentrate on discussing those observations of waves trapped to more discrete features, especially the Hawaiian Islands and the Juan de Fuca ridge segment. Waves trapped to seamounts, which have been found to reach amplitudes up to 40 cm/s (*Eriksen*, 1991), are treated by other authors in this volume.

There are now quite a few observations of narrow-band (in frequency) wave motions that appear to be resonances of the oceanic fluid system in the presence of discrete topographic features. These resonant waves are the most easily identifiable members of the whole class of oscillations which can exist at discrete topography, but are just a small portion of this class. The resonance can occur because the wavelength of a particular wave neatly circumscribes the discrete topography in an integral number of wavelengths, or because the characteristic dispersion of the trapped oscillations admits a zero group velocity point in the (single) direction of propagation thus allowing energy to accumulate. Perhaps what is most remarkable about these resonances is their existence at all, and especially their existence as underdamped oscillations in the presence of highly irregular topography that intuitively would be expected to cause strong damping. As will be seen, the irregular topography of such features as mid-ocean ridges does not seem to inhibit the existence of resonances which necessarily have been studied with only the smoothest of ideal geometries.

The resonant oscillations are easy to study, and have been studied with datasets not specifically intended for that purpose, because their amplification at discrete fre-

quencies makes them identifiable in autospectra of oceanic variables taken at widely separated locations, and, because being narrow-band in frequency usually implies small wavenumber bandwidth, leading to relatively high horizontal coherence. Thus it is easier to describe these phenomena from a sparse array of instruments than it is to describe broad-band phenomena.

An important practical consequence of narrow-band resonance among trapped waves is that the resonant waves are reservoirs of energy well above what would be present at the topographic boundary due to ambient open ocean variability. Such reservoirs must have an impact on mixing at the boundaries, or on dispersal of the products of such mixing, especially since the trapped waves tend to have their largest amplitudes right at the boundary. If you subscribe to the idea that sub-thermocline mixing occurs at water-earth boundaries (Gilbert and Garrett, 1989), then at mid-depth levels (2000m - 3000 m) in the ocean you have to be concerned about what motions exist along the ~50,000 km of mid-ocean ridge crests. Irrespective of a role in global mixing, the resonant oscillations definitely play a role in the redistribution of anthropogenic and hydrothermal effluents (e.g., Cannon *et al.*, 1991), as will be clear from the following examples. It is also clear that non-linear advection can result in strong residual currents, as already demonstrated by observations (Eriksen, 1991) and numerical simulations (Haidvogel *et al.*, 1993) of resonant waves at seamounts.

Killworth (1989a) has emphasized the importance of topographic waves in extracting energy from coastal Kelvin waves (when the ridge intersects a coast). A logical extension of this idea is that ridge waves may be important sinks for open ocean Rossby wave energy. The implications for general circulation models which either don't have the horizontal resolution to resolve the various topographic wave modes or incorporate general Laplacian damping is that the shorter-scale topographic waves will be under-represented resulting in under-damping of the Kelvin or Rossby type motions.

On the following pages I will present examples of what appear to be resonant oscillations trapped to specific topographic features, including especially the Hawaiian Islands and the Juan de Fuca Ridge. The material presented is from both a review of the literature and ongoing research.

Considering that many topographic waves are physically distant from the sea surface and hence apparently isolated from the action of surface winds, investigation of how the waves are forced has led to some especially intriguing observations and speculations of new energy pathways or energy transfer mechanisms. Waves trapped to seamounts and ridges, for instance, that are evanescent upward still may be forced by atmospheric winds, either directly via the wind's establishment of forced oscillations that are evanescent downward from the surface but still intersect the topography (producing a "tunnelling" of energy from the surface to the topography),

Table 1. Examples of waves trapped to discrete topography

	Period	Characteristics	References
<u>Ridge Segments</u>			
Juan de Fuca Ridge (~46°N, 129°W)	4 days	baroclinic; trapped to ridge crest horizontally and vertically	Thomson (1989) Chave <i>et al.</i> (1989) Cannon <i>et al.</i> (1991) Allen and Thomson (1993)
Faroe-Iceland Ridge (~63°N, 10°W)	1.8 days	barotropic; trapped horizontally	Miller <i>et al.</i> (1995)
<u>Banks, Plateaus, Seamounts</u>			
Rockall Bank (~57°N, 14°W)	1 day	barotropic; trapped horizontally	Huthnance (1974)
Yermak Plateau (~82°N, 10°E)	1 day	barotropic; trapped horizontally	Hunkins (1986)
Fieberling Guyot (~32°N, 128°W)	1 day	baroclinic; bottom trapped; rectification observed	Eriksen (1991) Noble <i>et al.</i> (1994)
<u>Islands</u>			
Bermuda Is. (~32°N, 65°W)	10 hrs to 17 dys	baroclinic; Kelvin Wave analogue	Wunsch (1972a) Hogg (1980) Eriksen (1982)
Hawaiian Is. (~21°N, 157°W)	17 hrs to 5 dys	baroclinic; Kelvin Wave analogue	Luther (1985) Lumpkin (1995)
Kerguelen Is. (~49°S, 70°E)	1.5 dys	barotropic; shelf wave analogue	Saint-Guilly and Lamy (1988)

or indirectly through generation of free barotropic waves which subsequently propagate into the region of a ridge. That the surface atmospheric fields do generate both evanescent and free barotropic waves at sub-inertial frequencies has been theoretically investigated (e.g., Frankignoul and Müller, 1979; Müller and Frankignoul, 1981) and observationally confirmed (e.g., Luther et al., 1990; Chave et al., 1992). The intermediary oscillation could transmit the atmosphere's effects over long distances before exciting the topographic waves, as may occur with surface gravity wave excitation of trapped waves around the Hawaiian Islands. Finally, resonances on neighboring topographic features may co-oscillate after one or the other resonance has been excited, as the trapped waves around the Hawaiian Islands demonstrate. Examples of some of these phenomena will be presented in the following pages.

Some Examples of Waves Trapped to Discrete Topography

Table 1 summarizes characteristics of some oscillations that have been observed at discrete topographic features. This is not an exhaustive list, but it will give a flavor of the growing number of observations of such

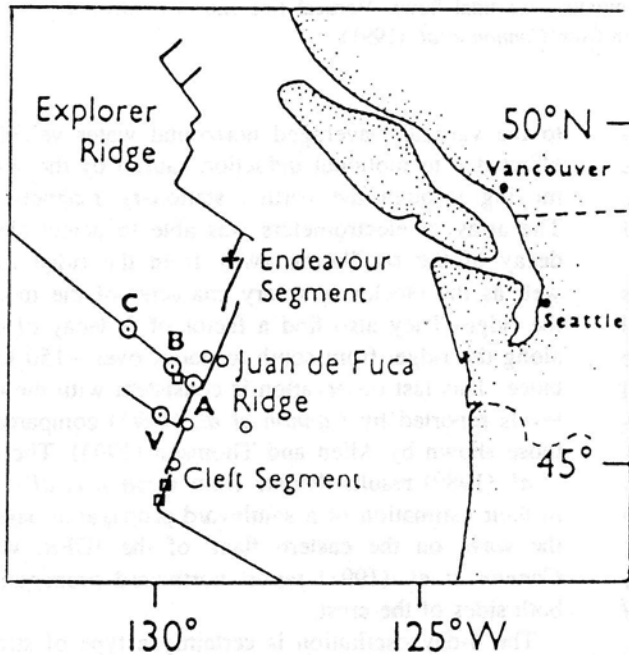


Figure 1. Line drawing of the Juan de Fuca Ridge and its segments. Three open squares show approximate locations of some of Cannon et al.'s (1991) moorings, including one between Axial and Brown Bear seamounts; the open circles indicate locations of five of Chave et al.'s instruments; and, the cross at the end of the Endeavour Segment locates the Thomson (1989) array. Circles with dots are seamounts: (A) Axial; (B) Brown Bear; (C) Cobb; and, (V) Vance. Figure modified from Cannon et al. (1991).

waves, and will provide some information on their salient features. Note that seamount trapped waves are treated in detail by other authors in this volume, and so will not be discussed further here. In this section, observations of waves trapped to the Juan de Fuca Ridge and to the Hawaiian Islands will be explored.

Ridge Waves

Cannon et al. (1991) describe several years of current and temperature observations from instruments moored at the southern end of the Juan de Fuca Ridge (JDFR) and at Axial Seamount in the middle of the ridge (Figures 1 & 2). Instruments near the ridge crest are dominated by a ~4-day oscillation that rotates predominantly clockwise (Figures 3 & 4). The oscillation is ubiquitous in all records in all years (Figure 4). The oscillation has maximum currents near the bottom in the rift valley. Near-bottom amplitudes are not uncommonly 10-15 cm/s (Figure 3). The currents decay upward and away (perpendicularly) from the ridge axis. Near the bottom the 4-day oscillation is more energetic than the

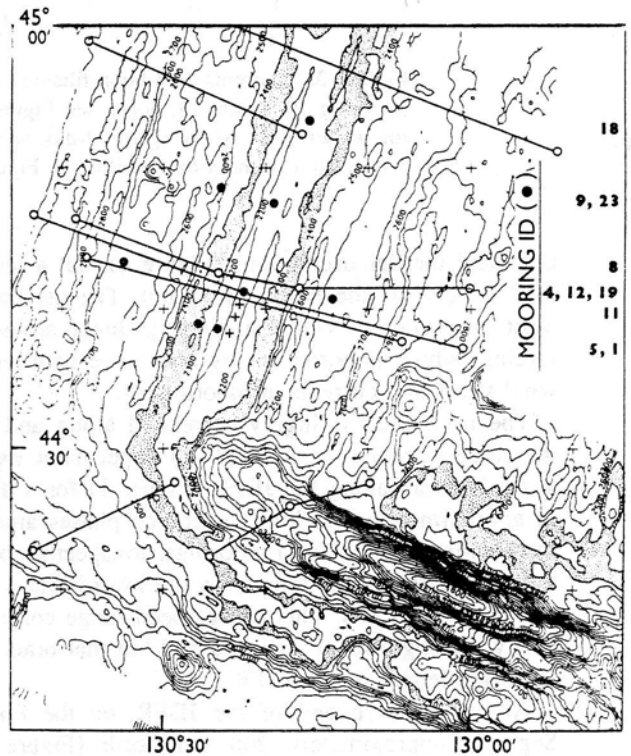


Figure 2. Chart of the southern end (the Cleft Segment) of the Juan de Fuca Ridge showing detailed locations of some of Cannon et al.'s (1991) moorings. Moorings are shown by solid circles with identification (ID) numbers on the right (4, 12, and 19 are at the same central location; 8 is on the west side; 11 is on the east side). Solid lines between open circles are conductivity-temperature-depth (CTD) sections. The contour interval is 100 m, and 2300-2400 m are stippled to better outline the ridge. Figure modified from Cannon et al. (1991).

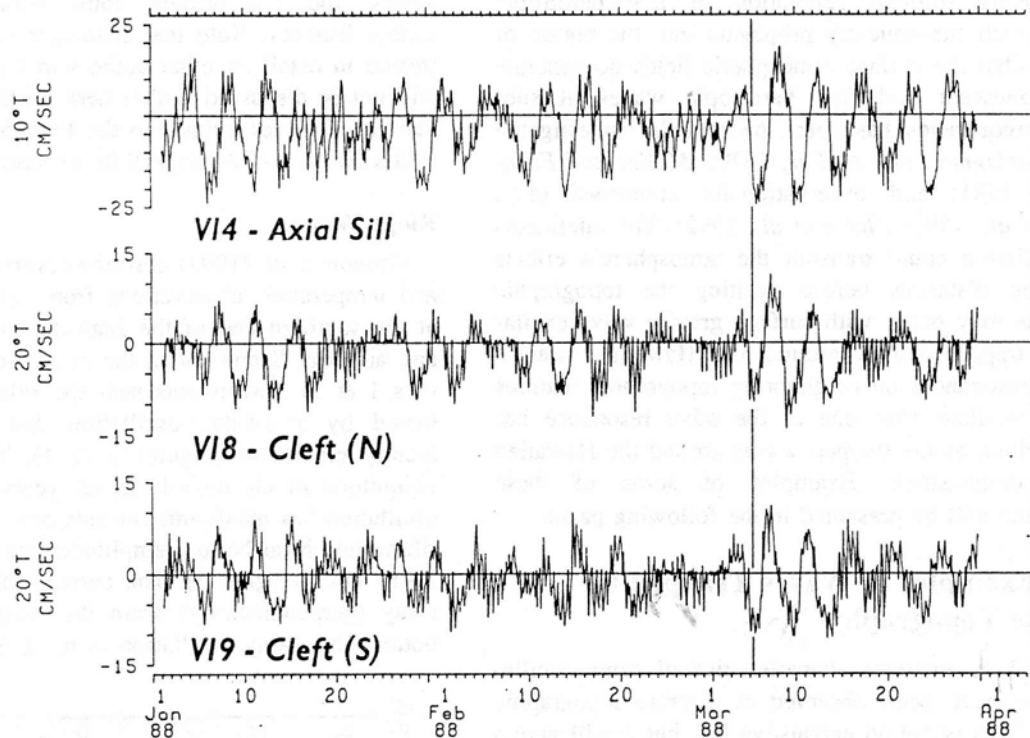


Figure 3. Currents (2.8-hour filtered) along 20° true in the rift valley of the Juan de Fuca Ridge (mooring 19, south; 18, north; see Figure 2) and across (10° true) the Axial-Brown Bear sill (Figure 1) for winter 1988, showing the 4-day signal dominating the tidal flows. Vertical line shows northward propagation of the 4-day oscillation. Figure taken from *Cannon et al.* (1991).

tides and inertial oscillations (Figure 4), but a few hundred meters off the bottom it is not. The oscillation is most energetic in winter suggesting direct atmospheric forcing, which is borne out by coherence between local wind stress and currents at mooring 19.

The oscillation is highly correlated along and across the ridge. *Cannon et al.*'s (1991) experiment extended about halfway along the JDFR (Figure 1) for a distance of approximately 150 km. Coherence phases among all the *Cannon et al.* (1991) moorings, irrespective of location across the ridge, indicate a northward phase propagation of 1-1.5 m/s. This phase speed range corresponds to a wavelength range of ~350-500 km that brackets the ~450 km length of the JDFR.

At the northern end of the JDFR, on the Endeavor Segment approximately 200 km north (Figure 1) of *Cannon et al.*'s (1991) most northerly instruments, *Thomson* (1989) and *Allen and Thomson* (1993) report observations of a 4-day oscillation with the same characteristics (such as clockwise polarization, amplification near the ridge crest, and vertical trapping) as reported by *Cannon et al.* (1991).

Chave et al. (1989) report observations of the 4-day oscillation in measurements of the horizontal electric field made on and near the JDFR. At periods greater than 1 day, the horizontal electric field is proportional

to the vertically-averaged horizontal water velocity, an effect due to motional induction caused by the seawater moving through the earth's stationary magnetic field. The array of electrometers was able to detect clearly a decay of the oscillation away from the ridge axis, as well as the clockwise rotary character of the motion at the ridge. They also find a factor of 3 decay of energy along the ridge, from south to north, over ~150 km distance. This last observation is consistent with the energy levels reported by *Cannon et al.* (1991) compared with those shown by *Allen and Thomson* (1993). The *Chave et al.* (1989) results deviate from *Cannon et al.*'s (1991) in their estimation of a southward propagation speed for the wave on the eastern flank of the JDFR, whereas *Cannon et al.* (1991) report northward propagation on both sides of the crest.

The 4-day oscillation is certainly a type of stratified, topographic oscillation. *Allen and Thomson* (1993) have simulated many of the characteristics (e.g., clockwise polarization, bottom and ridge crest trapping) of the oscillation with a forced model under the assumption of no along-ridge variability. *Killworth* (1989a, 1989b) has performed the most complete analysis to date of the potential suite of free oscillations trapped to a ridge, but necessarily restricted his model to no more than two fluid layers to retain a certain amount of analytical trac-

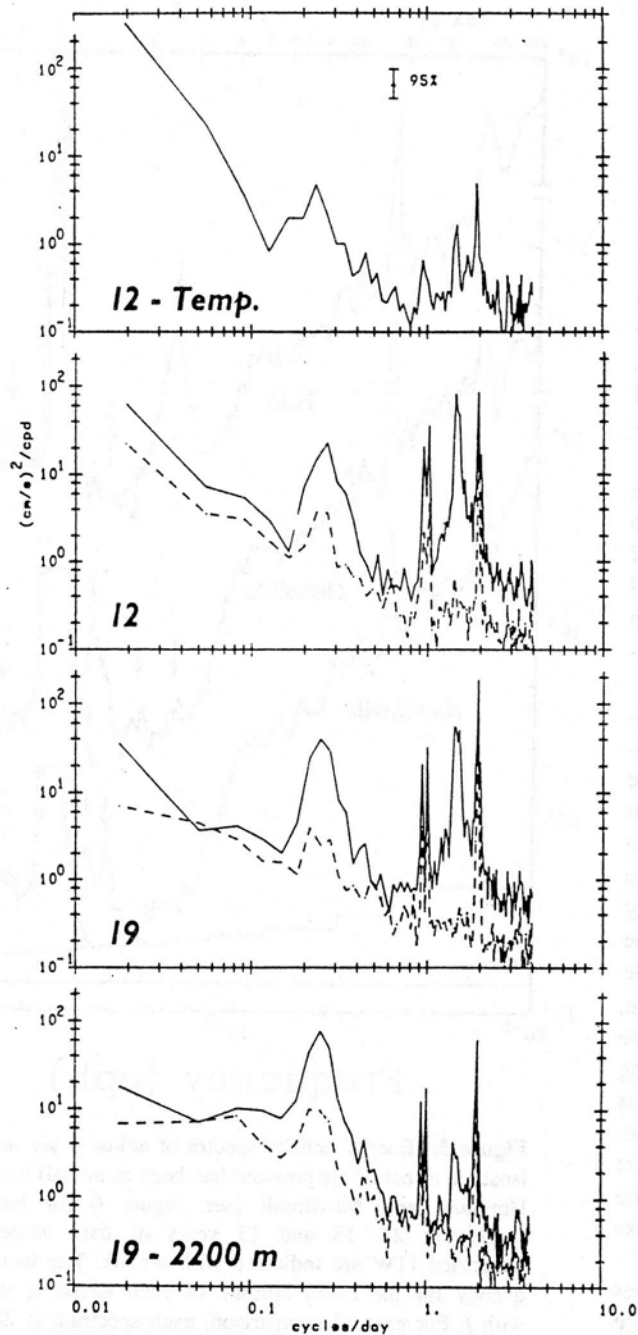


Figure 4. From top to bottom, auto-spectral densities for temperature at 2000 m at mooring 12, currents at 2000 m at mooring 12, currents at 2000 m at mooring 19, and near-bottom currents at 2200 m at mooring 19. Mooring 12 was deployed in 1986-1987, while mooring 19 was deployed in 1987-1988. For the currents, the solid curve is clockwise. Confidence limits of 95% are shown for 24 degrees of freedom. Figure taken from Cannon *et al.* (1991).

tability. Even so, Killworth's models provide enough information on wave structure and dispersion to speculate as to why the JDFR 4-day oscillation is resonant, and why there might be different phase propagation directions at different distances from the ridge.

Many of the solutions presented by Killworth have very asymmetric structures. That is, they have very large amplitudes only at the crest and on one side of the ridge, i.e., the side where the ridge crest is to the right of the direction of propagation (northern hemisphere case). One can then readily imagine that oscillations could propagate north along the west side of the JDFR and south along the east side. Reinforcement, that is resonance, occurs when the distance of a transit around the ridge equals an integral number of along-isobath wavelengths of the oscillation. The gravest mode (mode 1) would have a wavelength equal to twice the length of the JDFR. The second gravest resonant mode (mode 2) would have a wavelength equal to the length of the JDFR, and so on. Cannon *et al.*'s (1991) phase speed measurements could correspond to a mode 2 wave, while Chave *et al.*'s (1989) measurements suggest mode 1. (N.b., Chave *et al.* (1989) point out that their phase speed estimate is uncertain to about a factor of 2, so that their 3 m/s speed is not significantly different from Cannon *et al.*'s (1991) 1.5 m/s speed; Chave *et al.* (1989) definitely observe southward propagation.)

It is remarkable that such a resonance should occur along the JDFR in the presence of that ridge's highly irregular topography. Figures 1 & 2 only give a scant indication of the true complexity of the topography. Notice that the JDFR is not even a single continuous ridge, but has several discontinuities (offsets) along its length. As will be shown below, resonant waves exist trapped to, and propagating around, highly irregular island topogeometries, as well.

An appealing way to reconcile the existence of a resonance with the complicated structure of the JDFR is to argue that, for a specific frequency and along-ridge wavenumber, zero group velocity along the ridge permits an accumulation of energy. In this case, one imagines the resonant character of the wave as being determined not by whether a complete circuit of the topography can be circumnavigated by the wave, but by the existence of a group velocity zero point on the frequency-wavenumber dispersion curves that permits local accumulation of energy at a particular frequency. Then every small segment of the JDFR can have its own zero group velocity point, and, since the cross-ridge profile of these segments is nearly the same, they could all have resonances at approximately the same frequency, and hence excitation of a resonance at one location could spread down the ridge.

The dispersion characteristics of the waves explored by Killworth (1989a, 1989b) have particular frequencies

and along-ridge wavenumbers where the along-ridge group velocities are zero, which would then permit the accumulation of energy, as for instance is the case for equatorially-trapped internal gravity waves (Wunsch and Gill, 1976). There would still be phase propagation, and given the structures calculated by Killworth, there could easily be two oscillations at the same ridge segment with exactly the same frequency and exactly the same along-ridge wavelength, but which have phase propagation in opposite directions and are therefore relatively isolated from each other because their amplitudes are strongest on opposite sides of the ridge. This scenario, then, could also explain the observations of northward propagation on the west side of the JDFR and southward propagation on the east side.

What is not explained by either scenario above is the apparent dominance of northward propagation at the top of the ridge in Cannon *et al.*'s (1991) observations. Of course, for the zero group velocity resonance, one could argue that the wave with northward phase propagation is stronger for some reason than the southward propagating wave.

The difference between the two scenarios of resonance above is more than an esoteric thought experiment. Whether energy propagates readily along the ridge directly relates to the major introductory point about whether the effects of forcing at one location on a mid-ocean ridge can travel far from the source. If the resonance on the JDFR is due to a wave propagating energy along the JDFR, then we can conclude that the substantial topographic irregularities do not impede propagation of these mesoscale waves along the ridge, hence we could expect to see disturbances propagate reasonably rapidly for thousands of kilometers along ridge crests. If, however, the resonance on the JDFR is due to zero group velocity, then the question of whether any ridge waves can propagate very far along a ridge is left unanswered, although diffusion of the energy of the resonance along the ridge is still possible through leakage to resonant waves on neighboring ridge segments.

Irrespective of this issue of whether or not the waves propagate energy along the ridges, the JDFR resonance demonstrates the existence of non-trivial ridge-trapped oscillations, which has a number of important local implications as outlined in the introduction.

Island-Trapped Waves (ITW)

Using sea level data, Luther (1985) showed that both sub-inertial and super-inertial waves are trapped to individual islands of the Hawaiian group. A few of the modes identified by Luther (1985) are indicated in sea level power spectra in Figure 5. That these oscillations can be associated with substantial current amplitudes is demonstrated in Figure 7. Luther (1985) established that the sub-inertial trapped oscillations were baroclinic,

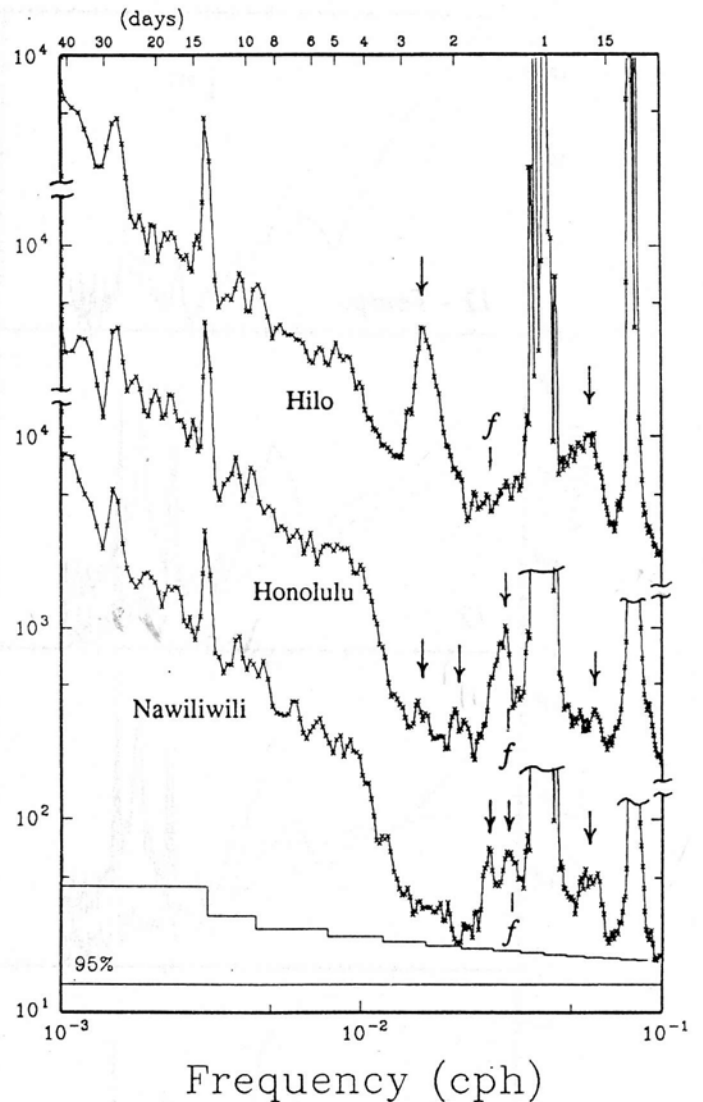


Figure 5. Energy density spectra of adjusted sea level (the isostatic effect of air pressure has been removed) from Hilo, Honolulu and Nawiliwili (see Figure 6 for locations), employing 24, 18 and 13 years of data, respectively. Suspected ITW are indicated with arrows. The inertial frequency for the mean latitude of each island is indicated with f . For ease of comparison, each spectrum is displaced from its neighbors by one decade along the ordinate. The diurnal and semi-diurnal tidal peaks in the Honolulu and Nawiliwili spectra have been clipped to simplify the figure. The fortnightly and monthly tides are clearly evident. The 95% confidence intervals at the bottom of the figure are exact for Nawiliwili but are slightly large for the other spectra. An increasing averaging bandwidth results in a decreasing confidence interval as frequency increases. The confidence intervals apply to each independent point. Every other point plotted is independent. The ordinate is in units of $(\text{cm})^2/\text{cph}$.

Kelvin-like trapped waves as first described by Wunsch (1972a) at Bermuda. The dynamics of the super-inertial modes are still unknown.

The potential impact of ITW on horizontal dispersion near Hawaii is suggested by Figure 8; band-passed currents (integrated over time) are shown in four frequency bands, including the sub-inertial band encompassing the gravest ITW mode around the island of Hawaii. Assuming the integrated currents emulate the Lagrangian drift of fluid particles, trapped waves were responsible for advection over 6 km compared to 2 km for inertial, diurnal and semi-diurnal motions.

Since baroclinic modes other than the first have little sea level deflection (unless the higher modes are substantially more energetic than the first), Luther (1985) necessarily only found clear evidence for first baroclinic modes, with a hint of a couple of second baroclinic modes. At Oahu, for instance, power spectral peaks at 1.5 days and 2 days (Figure 5) correspond to peaks in coherence amplitude between sea level stations on opposite sides of the island (Figure 9). The coherence phase at these periods is not significantly different (at the 95% level) from what would be expected ($\sim 105^\circ$) for an azimuthal mode 1 wave propagating clockwise around the island as appropriate for Kelvin waves. Luther (1985) concluded that the 1.5 day oscillation was the 1st baroclinic, 1st azimuthal ITW mode for Oahu and that the 2 day oscillation was the 2nd baroclinic, 1st azimuthal mode.

At Bermuda, where sea level deflections of the modes are not at all robust (compare Wunsch's, 1972b, Figure 2 with Figure 5 here), Hogg (1980) observed modes as high as the 4th baroclinic in current meter data. For the island of Hawaii, the 4th baroclinic, 1st azimuthal mode would have a period of approximately 8 days, assuming the validity of the cylindrical model for computing the resonant periods. Hogg (1980) also speculated that strong coherence among current meter records at ~ 17 days may be due to an island or topographically trapped oscillation. This information is presented simply to indicate the potential range of periods for which trapped waves may provide a significant amount of the nearshore variability.

Figure 10 shows power spectra of azimuthal velocity taken from a mooring (C10 in Figure 6) near the island of Hawaii. A clear peak at 2.7 days period is seen at 54 m and 363 m. This is probably the 1st baroclinic, 1st azimuthal mode identified by Luther (1985) and seen in Figure 5 (top). At the deepest depth available (771 m), the 2.7-day peak is no longer evident, but a peak at 4.5 days is seen. Whether this longer period peak represents a higher baroclinic trapped mode(s) is the subject of current research. At the moment, the cause of the 4-5 day peak at 771 m in Figure 10 is suspected to be that, at this depth, the graver baroclinic/radial modes with smaller periods are relatively weaker than the higher baroclinic/radial modes with longer periods. Our intuition on this point comes from the results of Brink

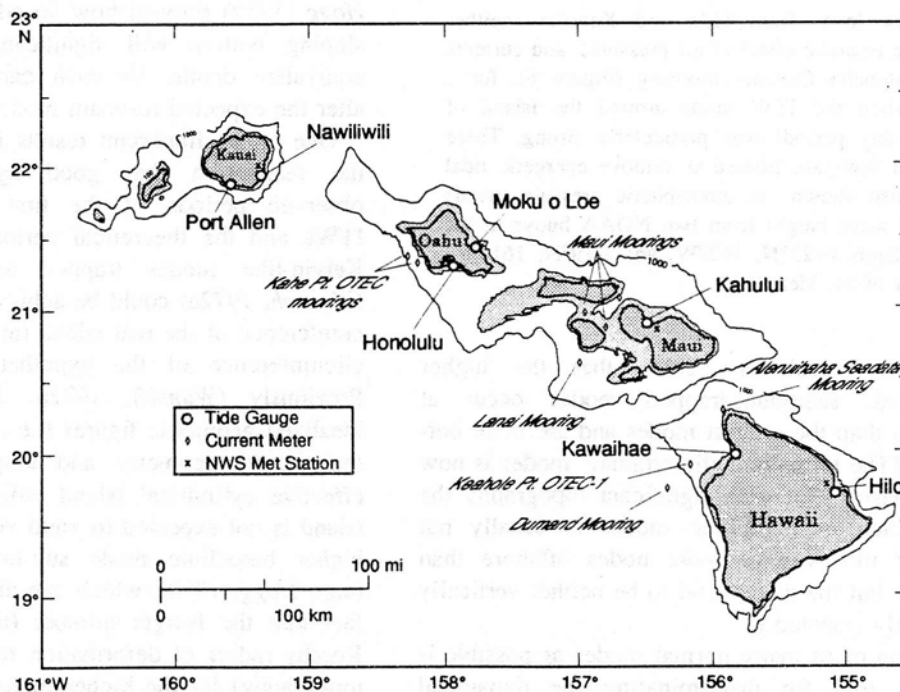


Figure 6. Map of the Hawaiian Islands showing locations of sea level and meteorological stations and current meter mooring sites, not all of which are mentioned in the text. Dark shading is land; light shading defines the 100 m isobath. The 1000 m isobath is also shown. Figure taken from Lumpkin (1995).

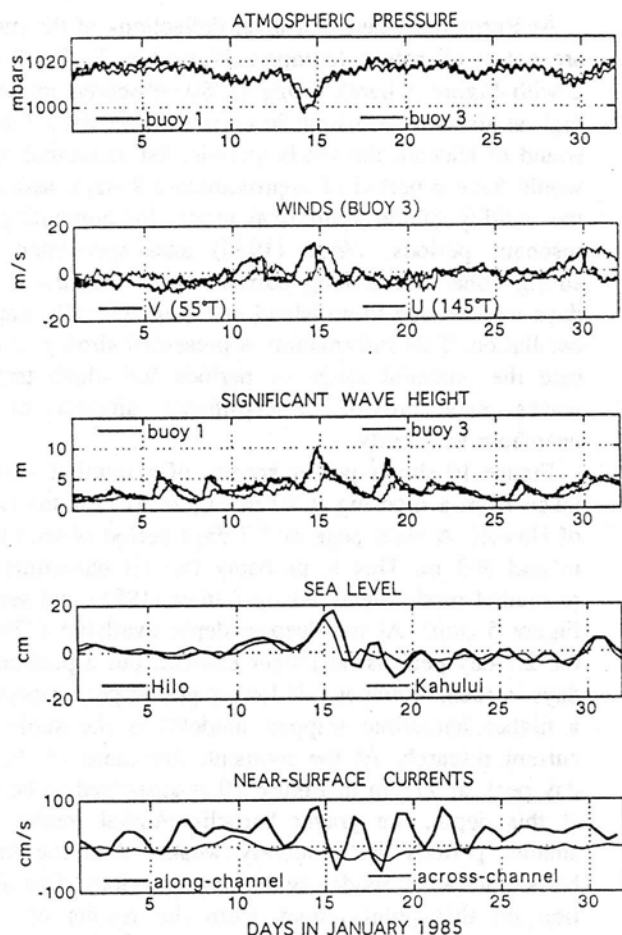


Figure 7. Sea level from Hilo and Kahului (neither adjusted for the isostatic effect of air pressure), and currents from the Alenuihaha Channel mooring (Figure 6), for a time period when the ITW mode around the island of Hawaii (~ 2.5 day period) was particularly strong. These data have been low-pass filtered to remove energetic tidal fluctuations. Also shown are atmospheric pressure, winds and significant wave height from two NOAA buoys to the west of the islands ($\sim 23^\circ\text{N}$, 162°W , and $\sim 19^\circ\text{N}$, 161°W). Figure courtesy of M. Merrifield.

(1989), whose calculations show that the higher baroclinic/radial, seamount-trapped modes occur at longer periods than the gravest modes and are more bottom trapped. [The term "baroclinic/radial" modes is now used to emphasize that with significant topography the classic definition of baroclinic modes is usually not valid. Higher modes have more nodes offshore than graver modes, but the nodes tend to be neither vertically nor horizontally oriented.]

Identification of as many normal modes as possible is an important tool for discriminating the dynamical appropriateness of models of variability around the islands, akin to the discrimination of earth structure models by the enumeration of normal modes of the earth (e.g., Gilbert and Dziewonski, 1975). For instance,

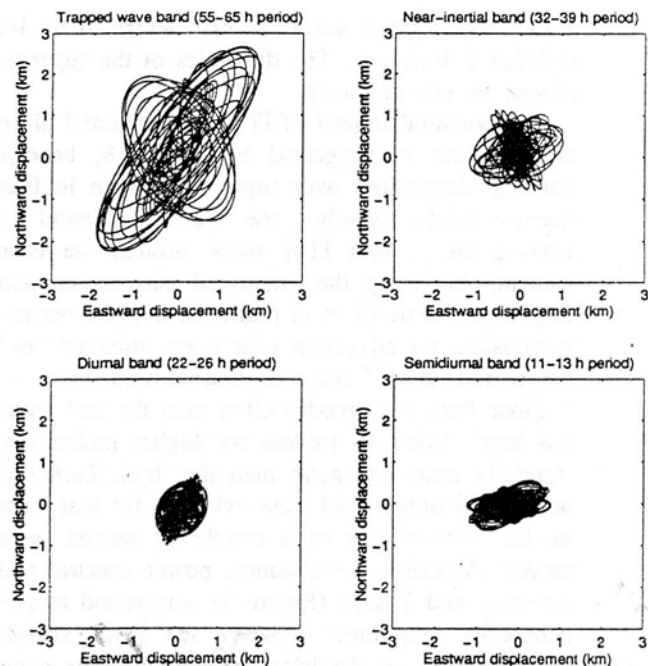


Figure 8. Progressive vector plots of the currents at 54 m at the Keahole Pt. OTEC-1 site, off the leeward coast of the island of Hawaii (Figure 6). Band-passing has isolated the motion at 55-65 h period (top left), 32-39 h period (top right), 22-26 h period (bottom left) and 11-13 h period (bottom right). The 55-65 h band encompasses the gravest ITW mode around the island of Hawaii. Figure taken from Lumpkin (1995).

Hogg (1980) showed how an ad hoc incorporation of a sloping bottom will significantly alter the expected equivalent depths for each baroclinic mode and thus alter the expected resonant mode periods.

One of the important results from Luther (1985) was the realization that good agreement between the observed periods of the first baroclinic sub-inertial ITWs and the theoretical periods of simple baroclinic Kelvin-like modes trapped to a cylindrical island (Wunsch, 1972a) could be achieved by matching the circumference of the real island (at the 20m isobath) to the circumference of the hypothetical cylindrical island. Previously (Wunsch, 1972a; Hogg, 1980), arbitrary idealized geometric figures (i.e., ellipses) were fit to the real island geometry and employed to estimate an effective cylindrical island radius. But, the cylindrical island is not expected to yield very useful predictions of higher baroclinic mode sub-inertial ITW frequencies (e.g., Hogg, 1980), which can also be deduced from the fact that the Burger number (the ratio of the internal Rossby radius of deformation to the radial scale of the topography) for the higher modes is relatively small. In other words, based on Hogg's (1980) work and Brink's (1989) study of seamount-trapped waves, it is certain that the dynamics of the ITW is non-trivially dependent upon topography, especially for the higher

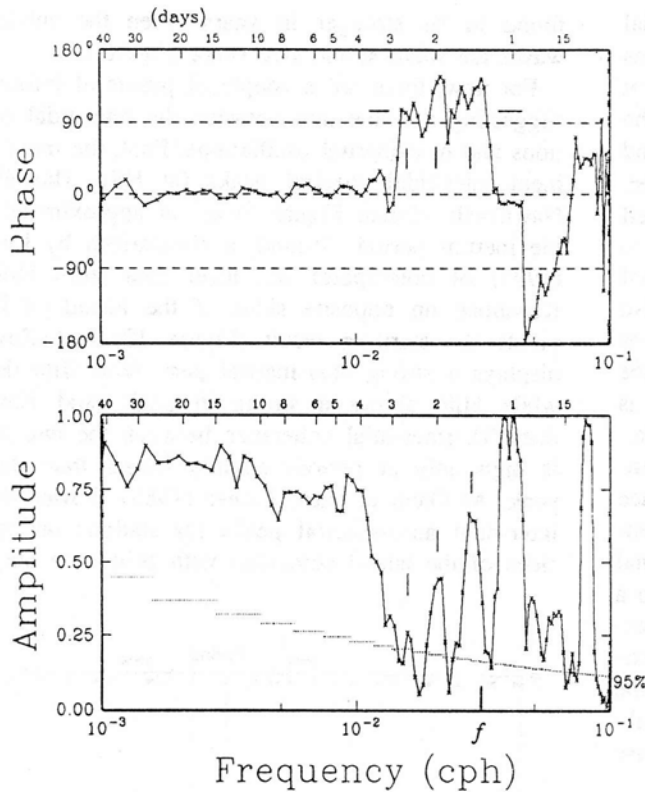


Figure 9. Coherence amplitude and phase between 8 years of adjusted sea level (isostatic effect of air pressure has been removed from the sea level) from Honolulu and Moku o Loe on the island of Oahu (Figure 6). High coherence amplitude is seen at the diurnal and semi-diurnal tidal frequencies. The high coherence amplitude with zero phase at periods greater than 3 days is due to open ocean barotropic oscillations. High coherence amplitude at 1.5 and 2 days is due to the 1st and 2nd baroclinic ITW modes around Oahu, respectively, both of which have auto-spectral peaks in Figure 5. The coherence phase at these periods is not significantly different from the -105° expected for an azimuthal mode 1 clockwise-propagating wave. A possible third baroclinic mode at about 2.7 days is also highlighted in this figure and Figure 5. The inertial frequency for the mean latitude of Oahu is indicated with f . The 95% level of no significance is indicated with a dotted line.

baroclinic/radial modes. However, given the success of mapping a real island to a cylindrical one, it is likely that a simple improvement of the model can yield reasonably good agreement with observations. That simple improvement is to include a radially-dependent, but azimuthally-invariant topography. The modal structures and frequencies can be obtained by resonance iteration, in a straight-forward adaptation of *Brink's* (1989) calculation of stratified-topographic, seamount-trapped waves. *Brink* has recently modified his code for this purpose.

The power spectra in Figure 5 clearly suggest the existence of narrow-band, super-inertial oscillations at frequencies between the diurnal and semi-diurnal tides

at each of the islands. *Luther* (1985) concluded, on the basis of coherence between sea level stations (Honolulu and Moku o Loe) on opposite sides of Oahu, that the inter-tidal peaks at the Oahu stations were due to oscillations propagating around the island that were probably trapped. He suggested that *Wunsch's* (1972a) theory of pseudo-resonant trapped waves might explain the peaks, as it did for super-inertial peaks at Bermuda. *Wunsch* (1972a) studied the reflection of an internal plane wave from a cylindrical island and found that at certain frequencies nearshore amplification occurred; he called this amplification a pseudo-resonance since there is not a true trapping of the wave around the island, i.e., free internal gravity waves exist at all frequencies to carry the energy away from the island. *Lumpkin* (1995) has evaluated the full *Wunsch* (1972a) solution with parameters appropriate for the Hawaiian Islands and has found that, for any reasonable choice of baroclinic and azimuthal mode numbers (i.e., less than 25 for each), the pseudo-resonances always occur closer to the inertial frequency f than $1.25f$, whereas the inter-tidal peaks in Figure 5 occur at approximately twice the inertial frequency (at about 17 hours period). [N.b., the phase lags found by *Luther*, 1985, suggest by Occam's razor an azimuthal mode number less than 4.]

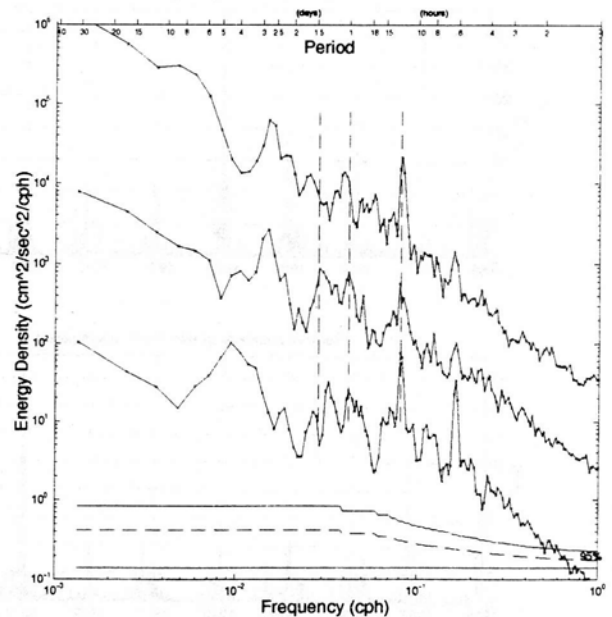


Figure 10. Azimuthal velocity spectra for 109-day long current records from the Keahole Pt. OTEC-1 site: 54 m (top), 363 m (middle) and 771 m (bottom). The 54 m (771 m) spectrum has been displaced up (down) one decade for viewing convenience. The sub-inertial peaks in the 54 m spectrum are at 2.8, 2.2 and 1.6 days period. Peaks in the 363 m spectrum are at 4.0, 2.8, 2.2 and 1.9 days period. The 771 m spectrum peaks at 4.4, 2.2 and 1.6 days period. The vertical dashed lines mark the inertial, diurnal and semi-diurnal periods. Figure taken from *Lumpkin* (1995).

Furthermore, if it is assumed that the inter-tidal waves that are showing up in the sea level observations at each island have the same horizontal phase speed, it is hard to imagine how they could produce nearly the same resonant frequency at islands like Kauai and Hawaii whose circumferences differ by a factor of three. (The resonant frequencies of the sub-inertial trapped waves after all - Wunsch, 1972a - are directly related to island size.) With similar periods of the super-inertial modes at each island, the differing island sizes also seem to rule out a refractively-trapped explanation, as might occur due to the sloping topography around the islands. However, if the oscillation is baroclinic it is hard to imagine that the topography doesn't play a role.

A relationship has been sought between the frequencies of the inter-tidal oscillations and sum or difference frequencies of the prominent tidal and inertial frequencies. The inter-tidal oscillations have a strong seasonal dependence (e.g., Figure 11 and Luther, 1985) and so a connection with the tides is unlikely. Despite the seasonal dependence, no coherence with atmospheric variables has been detected. Interannual dependence of the wave's amplitude rules out a connection to the sub-inertial trapped waves, since the super-inertial waves are

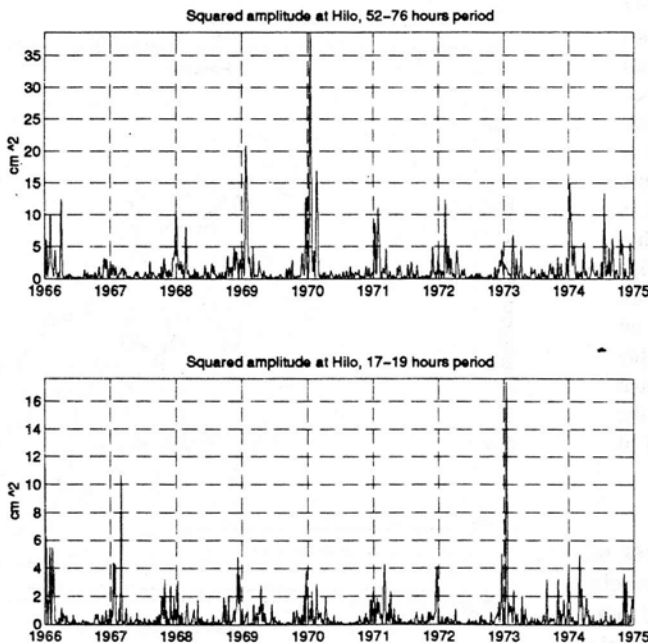


Figure 11. Variance of adjusted sea level from Hilo, 1966-1974, obtained from a complex demodulation using a 5-point Butterworth IIR filter with a cutoff frequency yielding the equivalent bandpasses of 52-76 h (top) & 17-19 h. Note the seasonal dependence (highest variance in winter) for both the sub-inertial and super-inertial motions, but note that they do not have the same interannual dependence of variance, and are therefore not likely to be dynamically linked to each other. Figure taken from Lumpkin (1995).

found to be stronger in years when the sub-inertial waves are weakest and vice versa (Figure 11).

For now, there are a couple of pieces of information suggesting a connection between the inter-tidal oscillations and near-inertial oscillations. First, the most prominent inter-tidal spectral peaks (at Hilo, Hawaii, and Nawiliwili, Kauai; Figure 5) are at approximately half the inertial period. Second, a comparison by Lumpkin (1995) of cotemporal sea level data from Hilo and Kawaihae on opposite sides of the island of Hawaii yields the startling result (Figure 12) that Kawaihae displays a strong near-inertial peak (and Hilo doesn't) while Hilo shows a strong $2f$ peak (and Kawaihae doesn't). Inter-tidal coherence between the two stations is high only at periods slightly longer than the Hilo peak. At Oahu at least, Luther (1985) showed that the inter-tidal auto-spectral peaks for stations on opposite sides of the island coincided with coherence amplitude

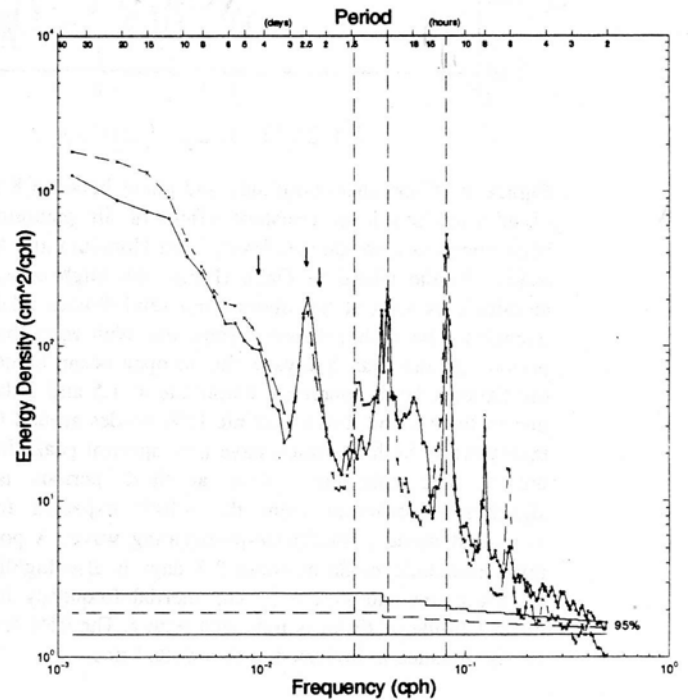


Figure 12. Adjusted sea level spectra for Hilo (solid) and Kawaihae, both on the island of Hawaii, for the same 3.5 year time period. The major tidal constituents have been analyzed and subtracted. Arrows indicate the theoretical periods of the first baroclinic, first azimuthal (center) and second baroclinic, first azimuthal (left) and second azimuthal (right) ITW modes. The vertical dashed lines mark the inertial, diurnal and semi-diurnal periods. Both spectra have an impressive sub-inertial peak centered at 2.5 days period, corresponding to the gravest ITW mode. The Kawaihae record has a near-inertial (super-inertial) peak at 1.4 days period which is not present at Hilo; an inter-tidal peak in the Hilo spectrum reaches its maximum at ~17.9 hours, but is not seen at Kawaihae. Figure from Lumpkin (1995).

peaks with significantly non-zero phase lags that indicated propagation around the island.

The present state of our knowledge of the dynamics of the narrow-band, super-inertial oscillations observed at the Hawaiian Islands is quite unsatisfactory. Furthermore, unlike the sub-inertial ITW which have been shown to be associated with significant currents, no such correspondence has yet been found for the super-inertial waves. They remain a curiosity, but whether they are more than that is not known.

Forcing Mechanisms

Ridge Waves

The generation of bottom trapped oscillations, such as the seamount trapped waves and the ridge waves discussed earlier, has been considered in some sense to be independent of the winds. For instance, regarding the forcing of seamount trapped waves, *Brink* (1990) has stated that it seems unlikely that such bottom-trapped features could be forced by surface wind stress effects. Rather, he suggests resonant excitation by ambient oceanic currents. Of course, this sidesteps the issue of what causes the "ambient oceanic currents." In fact, at periods from the inertial to 10 days in which the JDFR wave resonance occurs, the atmosphere readily forces oceanic currents (e.g., *Frankignoul and Müller, 1979; Müller and Frankignoul, 1981*) that are evanescent from the sea surface (at the shorter periods in this band) or barotropic free waves (at the longer periods). The evanescent oscillations tend to have large vertical decay scales so that they have non-negligible velocities at the seafloor. Therefore, the "ambient oceanic currents" needed to force waves trapped over bottom topographic features could be directly forced by the fluctuating winds (as opposed to being the result of mean current instability, for instance).

A potential flaw in this sequence of events is that the (barotropic or evanescent) currents forced by the fluctuating winds are not very energetic. *Luther et al. (1991)* and *Chave et al. (1992)* observed amplitudes of only $O(1 \text{ cm/s})$ for barotropic currents directly forced by the atmosphere in the mid-latitude North Pacific. But this simply emphasizes one of our points, that is, the existence of free waves trapped to topography, especially if the dynamics impose a resonance, permits local near-topography enhancement of the initial forcing amplitude. *Chapman (1989)* and *Haidvogel et al. (1993)* find amplification factors up to $O(100)$ times the strength of the incident barotropic current in analytical and numerical models of forcing of waves trapped to isolated topographic features.

Cannon et al. (1991) detected significant coherence between local wind stress and the 4-day oscillating

currents over the southern JDFR. In conjunction with the winter-time enhancement of the energy in this band that they and *Allen and Thomson (1993)* report, direct atmospheric forcing of the JDFR waves appears certain.

Island-Trapped Waves

Direct forcing by the wind is clearly capable of exciting at least the gravest sub-inertial ITW. Figure 11 exhibits a seasonal cycle in the energy of the gravest ITW mode around the island of Hawaii, which characteristic is generally interpreted as resulting from direct forcing by the atmosphere (*Wunsch, 1972a; Hogg, 1980*). Furthermore, Figure 13 shows significant coherence amplitude between adjusted sea level and north wind stress at the period of the gravest ITW around the island of Hawaii. The phase associated with this high coherence rapidly changes nearly 180° at the ITW period as expected for a forced resonance. This type of evidence of excitation of resonant ITW modes was also found by *Hogg (1980)* at Bermuda.

The simplest model of the wind forcing is to consider a flat-topped, cylindrical island with an imposed

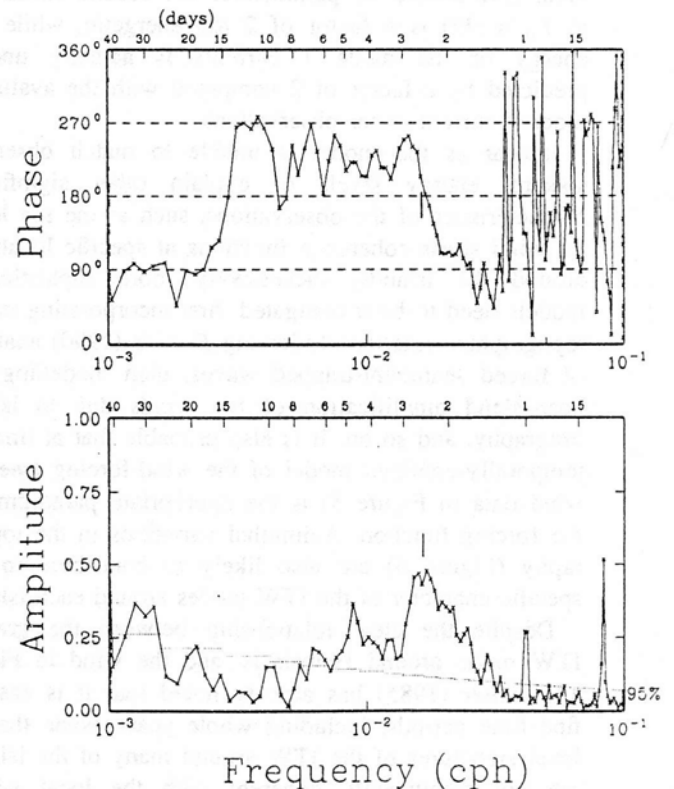


Figure 13. Coherence amplitude and phase between 24 years of adjusted sea level and north wind stress from Hilo. The period of the gravest sub-inertial ITW mode around the island of Hawaii is indicated by the short vertical lines in the amplitude and phase plots. Due to the highly significant coherence amplitude and the nearly 180° phase shift, the gravest ITW around Hawaii can be considered to be resonantly forced by the local wind field.

homogeneous, uni-directional, oscillating wind stress. Under these conditions it is easy to imagine that an azimuthal mode one ITW could be excited by the divergence of the wind-produced Ekman flux as it encounters the island. On one side of the island the horizontal flux divergence causes a set-down of the thermocline, and on the other side a set-up. Half a period later the set-down/set-up pattern is reversed, thus potentially reinforcing an azimuthal mode 1 wave that has propagated halfway round the island. The dynamics of this scenario has been qualitatively confirmed by Lumpkin (1995) with a simple analytical model that examines the model response as the forcing frequency varies. The normalized energy spectrum from this model is presented in Figure 14. The figure clearly displays the lower frequencies and shorter offshore decay scales of successively higher baroclinic modes. All the modes have an azimuthal wavenumber of 1, since the choice of forcing projects only onto that mode. Model parameters were chosen so that the maximum sea level energy density and frequency bandwidth of the gravest ITW mode matches the sea level spectrum at Hilo in Figure 5. With this choice of parameters, the second mode (at $\omega/f_0 = .35$) is a factor of 2 too energetic, while the energy of the mode 1 currents is actually under-predicted by a factor of 2 compared with the available moored current meter observations.

Insofar as the model is unable to match observed spectral energy levels or explain other significant characteristics of the observations, such as the sea level vs. wind stress coherence functions at specific locations around the islands, successively more sophisticated models need to be investigated, first incorporating radial topographic variations following Brink's (1990) analysis of forced seamount-trapped waves, then modelling the near-island amplification of the winds due to island orography, and so on. It is also probable that at times a temporally-confined model of the wind-forcing (see the wind data in Figure 5) is the appropriate paradigm for the forcing function. Azimuthal variations in the topography (Figure 6) are also likely to contribute to the specific character of the ITW modes around each island.

Despite the clear relationship between the gravest ITW mode around Hawaii Is. and the wind in Figure 13, Luther (1985) has already noted that it is easy to find time periods, including whole years, when the sea level signatures of the ITW around many of the islands are not significantly coherent with the local winds. Luther (1985) has postulated two additional mechanisms of ITW forcing to account for this. First, due to the narrowness of the inter-island channels, it is possible that significant energy in an ITW mode around one island will leak (scatter, if you prefer) to a neighboring island, exciting a co-oscillation of that island's ITW modes. Lumpkin (1995) found, using time-dependent coherence functions (Figure 15), a number of time periods which

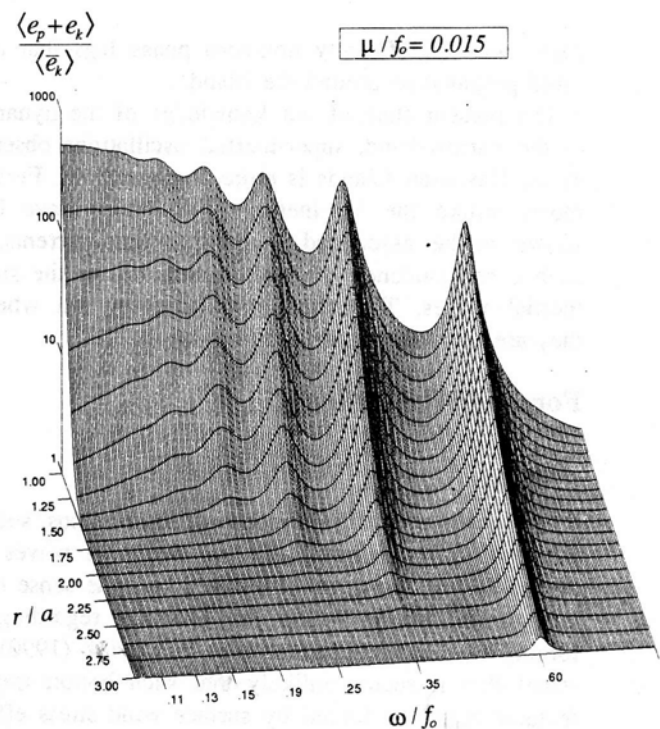


Figure 14. Total mean specific energy divided by mean background specific kinetic energy for the forced island-trapped wave model of Lumpkin (1995), with a dissipation time scale $\mu^{-1} = f_0 / 0.015$ (≈ 15.8 days). Frequencies from $\omega/f_0 = 0.1$ to $\omega/f_0 = 1$ (inertial) are shown; tick marks are at the inertial frequency and at the baroclinic eigenfrequencies. The energy ratio is given for radial distance r ranging from the island radius a to $3a$. Note that the trapping scale decreases for increasing baroclinic mode (decreasing frequency). Figure taken from Lumpkin (1995).

appear to clearly show such co-excitation of the Maui group's gravest ITW by Hawaii's gravest ITW, while also showing time periods when the gravest Hawaii Island ITW was strong and the Maui Island ITW was weak (e.g., winter of 1974), and vice versa (summer-fall of 1971). In both the latter cases, there is no coherence between the islands indicating that the individual islands do have separate resonances, although just why the leakage should not always occur is not immediately apparent. A multiple regression analysis of the Hilo and Kahului sea levels and local winds has confirmed that leakage from the island of Hawaii to Maui is more important than local wind forcing at Maui, although the latter does occur.

This is perhaps the first time such a co-oscillation phenomenon has been identified in the ocean. Quantification of this process, and the extent to which it occurs between other islands in the group is the subject of current research. This process may explain the existence of the 4-day oscillation all along the JDFR, despite the discontinuous nature of that ridge (Figure 1). That is, if the JDFR resonance is due to the excitation of waves that have zero along-ridge group velocity, the

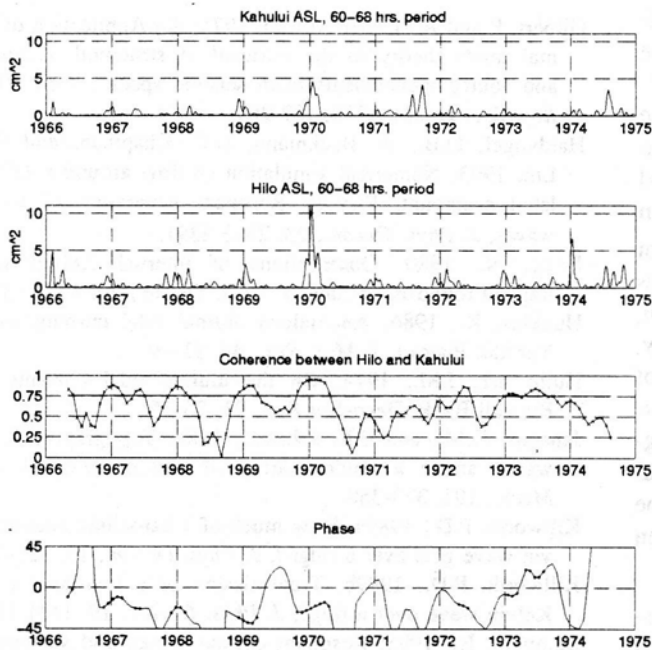


Figure 15. Bottom two frames, running coherence amplitude and phase between band-passed adjusted sea level records from Kahului and Hilo for the 2.5 to 2.83 days period band. The complex demodulated variance in this band for each station is presented in the top two frames. The coherence was calculated from the phase-bearing band-passed signals and not from the variance envelopes. The horizontal line at coherence amplitude 0.75 indicates the 95% confidence level. Figure from *Lumpkin* (1995).

similarity of the cross-ridge topographies for each small segment ensures that the resonant modes will all have the same frequencies. Then excitation of a resonant mode on one small ridge segment could result in co-oscillation of neighboring segments' resonant modes, and so on down the length of the JDFR. If one postulates a small amount of energy loss as this process occurs, the observation of south to north decay of energy in the 4-day oscillation discussed earlier could be explained.

Continuing in a speculative vane, as appropriate for this workshop presentation, note that *Luther* (1985) found a reasonable correspondence between the incidence of large tsunamis and ITW excitation at Hawaii. He postulated that the divergence of the radiation stress associated with a tsunami as it shoals would be sufficient to produce a substantial set-up/set-down profile of the thermocline (as well as of the sea surface), since the thermocline is relatively shallow and is relatively close to shore due to the steepness of the island topography. After the passage of the tsunami, when the stress divergence which maintained the thermocline set-up/set-down is gone, the thermocline profile will try to relax to its former position and this relaxation process should generate ITW. Such a sequence of events could also occur when large ocean swells hit the islands to

produce the huge surf for which Hawaii is famous (note the significant wave height in Figure 7).

It is only in the last ten years that adequate time series of surface gravity wave energy have become available to permit a better testing of the gravity wave excitation mechanism. And there is certainly sufficient wind data now to be able to isolate those time periods when local wind forcing could not be responsible for the ITW generation. Investigations with these data are in progress. If the surface gravity wave forcing of ITW is found to actually occur it will represent a new addition to the suite of mechanisms by which the atmosphere generates internal motions in the ocean.

In summary, it is easy to imagine that at times a broad-scale oscillating wind (possibly rotating anti-cyclonically) is responsible for significant sub-inertial ITW excitation, while at other times short-lived storm events, or surface gravity wave set-up/set-down, contribute significantly to the wave excitation. And then at other times wave energy at one island may be due to leakage from ITW modes around a neighboring island.

Final Remarks

There is sufficient observational evidence to conclude that energetic, resonant, baroclinic oscillations exist trapped to islands and mid-ocean ridges. The lowest order dynamics of these waves is known, but significant details remain un-determined, such as the specific role of topography for the ITW and the cause of the resonance of the JDFR waves. For the super-inertial oscillations at the Hawaiian Islands, even the lowest order dynamics is not known.

Direct atmospheric forcing of both ITW and ridge waves has been demonstrated. The former is most likely via divergence of the Ekman transport as it impinges on the island, and the latter may involve a "tunnelling" of energy from the surface to the topography if the frequency-wavenumber characteristics of the forcing do not permit the generation of free open-ocean Rossby waves. Indirect atmospheric forcing is postulated for ridge waves through the intermediary of Rossby or Kelvin waves, and for ITW through the intermediary of surface gravity waves.

The existence of resonant ridge waves engenders the notion of a whole class of waves capable of propagating information long distances along the mid-ocean's ridges. Their extraction of energy from non-topographic Rossby or Kelvin waves may be a significant sink of energy that, for instance, is poorly modeled in GCM's.

Both the ITW and ridge waves imply the existence of enhanced current amplitudes in the immediate vicinity of the topography. This variability may be important to oceanic mixing by intensifying boundary layer shears or improving the efficiency of removal of boundary-mixed water. The waves must certainly enhance the dispersal

of anthropogenic effluents at islands and hydrothermal effluents at mid-ocean ridges. In addition, both wave types may result in substantial rectified flows.

The concept of energy leakage, or forcing of one resonant trapped oscillation by a resonant oscillation trapped to a neighboring topographic feature, has good support from the observations of ITW at the Hawaiian Islands, and may be responsible for the diffusion of energy down the JDFR. However, this problem has many non-intuitive aspects (e.g., *Jansons and Johnson*, 1988; Hendershott, this volume). Most importantly, energy propagation through, for instance, an array of seamounts may not necessarily proceed in the straight-forward manner that previous discussions would suggest; that is, even if the seamounts have identical resonant frequencies, a resonance excited at one seamount need not spread equally to all the others, even if they are in close proximity.

Acknowledgments. This work benefited from discussions with R. Lumpkin, M. Merrifield and S. Allen. I am grateful to G. Cannon and R. Lumpkin for permitting the use of many of their figures.

References

- Allen, S.E., and R.E. Thomson, 1993: Bottom-trapped subinertial motions over midocean ridges in a stratified rotating fluid, *J. Phys. Ocean.*, 23, 566-581.
- Brink, K.H., 1989: The effect of stratification on seamount-trapped waves, *Deep-Sea Res.*, 36, 825-844.
- Brink, K.H., 1990: On the generation of seamount-trapped waves, *Deep-Sea Res.*, 37, 1569-1582.
- Brink, K. H., 1991: Coastal-trapped waves and wind-driven currents over the continental shelf, *Ann. Rev. Fluid Mech.*, 23, 389-412.
- Cannon, G.A., D.J. Pashinski, and M.R. Lemon, 1991: Mid-depth flow near hydrothermal venting sites on the southern Juan de Fuca Ridge, *J. Geophys. Res.*, 96, 12,815-12,831.
- Chapman, D.C., 1989: Enhanced subinertial diurnal tides over isolated topographic features, *Deep-Sea Res.*, 36, 815-824.
- Chave, A.D., J.H. Filloux, D.S. Luther, L.K. Law, and A. White, 1989: Observations of motional electromagnetic fields during EMSLAB, *J. Geophys. Res.*, 94, 14,153-14,166.
- Chave, A.D., D.S. Luther, and J.H. Filloux, 1992: The Barotropic Electromagnetic and Pressure Experiment, 1. Atmospherically-forced barotropic currents, *J. Geophys. Res.*, 97, 9565-9593.
- Eriksen, C.C., 1982: An upper ocean moored current and density profiler applied to winter conditions near Bermuda, *J. Geophys. Res.*, 87, 7879-7902.
- Eriksen, C.C., 1991: Observations of amplified flows atop a large seamount, *J. Geophys. Res.*, 96, 15,227-15,236.
- Frankignoul, C., and P. Müller, 1979: Quasi-geostrophic response of an infinite β -plane ocean to stochastic forcing by the atmosphere, *J. Phys. Ocean.*, 9, 105-127.
- Gilbert, D. and C. Garrett, 1989: Implications for mixing of internal wave scattering off irregular topography, *J. Phys. Ocean.*, 19, 1716-1729.
- Gilbert, F and A.M. Dziewonski, 1975: An Application of normal mode theory to the retrieval of structural parameters and source mechanisms from seismic spectra, *Phil. Trans. Roy. Soc. Lond.*, A278, 187-269.
- Haidvogel, D.B., A. Beckmann, D.C. Chapman, and R.-Q. Lin, 1993: Numerical simulation of flow around a tall isolated seamount. Part II: Resonant generation of trapped waves, *J. Phys. Ocean.*, 23, 2373-2391.
- Hogg, N., 1980: Observations of internal Kelvin waves trapped round Bermnuda, *J. Phys. Ocean.*, 20, 1353-1376.
- Hunkins, K., 1986: Anomalous diurnal tidal currents on the Yermak Plateau, *J. Mar. Res.*, 44, 51-69.
- Huthnance, J.M., 1974: On the diurnal tidal currents over Rockall Bank, *Deep-Sea Res.*, 21, 23-35.
- Jansons, K.M., and E.R. Johnson, 1988: Topographic Rossby waves above a random array of seamounts, *J. Fluid Mech.*, 191, 373-388.
- Killworth, P.D., 1989a: How much of a baroclinic coastal Kelvin wave gets over a ridge?, *J. Phys. Ocean.*, 19, 321-341.
- Killworth, P.D., 1989b: Transmission of a two-layer coastal Kelvin wave over a ridge, *J. Phys. Ocean.*, 19, 1131-1148.
- Lumpkin, R., 1995: Resonant coastal waves and superinertial oscillations, M.S. Thesis, U. Hawaii, Honolulu, HI, 106 pp.
- Luther, D.S., 1985: Trapped waves around the Hawaiian Islands, Proceedings of the 3rd Hawaiian Winter Workshop, L. Magaard (ed.), U. of Hawaii, Honolulu, HI, pp. 261-301.
- Luther, D.S., Chave, A.D., J.H. Filloux, and P.F. Spain, 1990: Evidence for local and nonlocal barotropic responses to atmospheric forcing during BEMPEX, *Geophys. Res. Lett.*, 17, 949-952.
- Luther, D.S., Filloux, J.H., and A.D. Chave, 1991: Low-frequency, motionally induced electromagnetic fields in the ocean: 2. Electric field and Eulerian current comparison, *J. Geophys. Res.*, 96, 12,797-12,814.
- Miller, A.J., P.F.J.G. Lermusiaux, and P.-M. Poulain, 1995: A 1.8-day topographic Rossby mode resonance trapped to the Iceland-Faroe Ridge, *Proc. 10th Conf. Atmos. Oc. Waves and Stability*, Big Sky, Montana, 5-9 June, 1995.
- Müller, P., and C. Frankignoul, 1981: Direct atmospheric forcing of geostrophic eddies, *J. Phys. Ocean.*, 11, 287-308.
- Noble, M.A., K.H. Brink, and C.C. Eriksen, 1994: Diurnal-period currents trapped above Fieberling Guyot: observed characteristics and model comparisons, *Deep-Sea Res.*, 41, 643-658.
- Philander, S.G., 1990: *El Niño, La Niña, and the Southern Oscillation*, Academic Press, New York, 289 pp.
- Saint-Guilly, B., and A. Lamy, 1988: Waves trapped by the Kerguelen Island escarpement, *C. R. Acad. Sci. Paris*, 307, II, 573-578.
- Thomson, R., 1989: Effects of topography and buoyant plumes on near-bottom currents over a mid-ocean ridge, *IEEE Oceans '89: The Global Ocean*, 1, 73-76.
- Wunsch, C., 1972a: The spectrum from two years to two minutes of temperature fluctuations in the main thermocline at Bermuda, *Deep-Sea Res.*, 19, 577-593.
- Wunsch, C., 1972b: Bermuda sea level in relation to tides, weather and baroclinic fluctuations, *Rev. Geophys. Sp. Phys.*, 10, 1-49.
- Wunsch, C., and A.E. Gill, 1976: Observations of equatorially trapped waves in Pacific sea level variations, *Deep-Sea Res.*, 23, 371-390.